

An Atomic Clock with 10^{-18} Instability

N. Hinkley,^{1,2} J. A. Sherman,¹ N. B. Phillips,¹ M. Schioppo,¹ N. D. Lemke,¹ K. Beloy,¹ M. Pizzocaro,^{1,3,4} C. W. Oates,¹ A. D. Ludlow^{1*}

¹National Institute of Standards and Technology, 325 Broadway, Boulder, CO 80305, USA. ²University of Colorado, Department of Physics, Boulder, CO 80309, USA. ³Istituto Nazionale di Ricerca Metrologica, Str. delle Cacce 91, 10135 Torino, Italy. ⁴Politecnico di Torino, Corso duca degli Abruzzi 24, 10125 Torino, Italy.

*Corresponding author. E-mail: ludlow@boulder.nist.gov

Atomic clocks have been instrumental in science and technology, leading to innovations such as global positioning, advanced communications, and tests of fundamental constant variation. Timekeeping precision at 1 part in 10^{18} enables new timing applications in relativistic geodesy, enhanced Earth- and space-based navigation and telescope, and new tests of physics beyond the Standard Model. Here, we describe the development and operation of two optical lattice clocks, both utilizing spin-polarized, ultracold atomic ytterbium. A measurement comparing these systems demonstrates an unprecedented atomic clock instability of 1.6×10^{-18} after only 7 hours of averaging.

Quantum mechanical absorbers like atoms serve as the best available time and frequency references: they are isolatable, possess well-defined transition frequencies, and exist in abundant identical copies. With over 50 years of development, clocks based on microwave oscillators referenced to atomic transitions now define the SI second and play central roles in network synchronization, global positioning systems, and tests of fundamental physics (1, 2). Under development worldwide, optical clocks oscillate 10^3 times faster than their microwave predecessors, dividing time into finer intervals (3). While microwave clocks like the Cs fountain have demonstrated time and frequency measurements of a few parts in 10^{16} (4, 5), optical clocks now measure with a precision of 1 part in 10^{17} (6–9).

A clock's instability specifies how its "ticking" fluctuates over time, a characteristic generally quantified by the Allan deviation (10). No time or frequency standard can make measurements better than the statistical precision set by its instability. Further, a clock's systematic uncertainty is often constrained by its long term instability. For these reasons, and because many timing applications require only exquisite instability, the instability represents one-if not the most-important property of an atomic standard.

In pursuit of lower instability, an optical lattice clock uses a stabilized laser referenced to many (10^3 to 10^6) alkaline-earth (or similar) atoms confined in an optical standing wave. Alignment of the clock interrogation laser along the direction of tight lattice confinement eliminates most Doppler and motional effects while probing the ultranarrowband electronic "clock" transition. These atoms are interrogated simultaneously, improving the atomic detection signal-to-noise and thus instability, which is limited fundamentally by quantum projection noise (QPN) (11). Like other cycled atomic clocks, the lattice clock suffers from a technical noise source known as the Dick effect, arising when an oscillator's noise is periodically sampled (12, 13). Cavity-stabilized lasers with low thermal noise have reduced the Dick effect, enabling clock instability below 10^{-15} at short times (14). Recently, an uncorrelated comparison of two strontium lattice clocks revealed clock instability of 3×10^{-16} at short times, averaging to 1×10^{-17} in 1000 s (8) or, in another case, reaching the 10^{-17} level in 20,000 s (9). Here, by comparing two independent optical lattice clocks using ultracold ^{171}Yb , we demonstrate a clock instability of 1.6×10^{-18} in 25,000 s.

Both clock systems, called here Yb-1 and Yb-2, independently cool and collect ^{171}Yb atoms from thermal beams into magneto-optical traps

[see Fig. 1 and (15)]. Two stages of laser cooling, first on the strong 1S_0 - 1P_1 cycling transition at 399 nm, followed by the weaker 1S_0 - 3P_1 intercombination transition at 556 nm, reduce the atomic temperature from 800 K to 10 μK . Each cold atom sample is then loaded into an optical lattice with $\sim 300E_r$ trap depth (recoil energy $E_r/k_B = 100$ nK) formed by retro-reflecting approximately 600 mW of laser power, fixed at $\lambda_m \approx 759$ nm (16) by a reference cavity. At the "magic" wavelength λ_m , both electronic states of the clock transition are Stark-shifted equally (17, 18). For the measurements described here, about 5000 atoms captured by each lattice are then optically pumped to one of the $m_F = \pm 1/2$ ground states using the 1S_0 - 3P_1 transition. After this state preparation, applying a 140 ms long π -pulse of 578 nm light resonant with the 1S_0 - 3P_0 clock transition yields the spectroscopic line-shape shown in Fig. 1C, with a Fourier-

limited linewidth of 6 Hz. Experimental clock cycles alternately interrogate both m_F spin states canceling first order Zeeman and vector Stark shifts. The optical local oscillator (LO) is an ultra-stable laser servo-locked to a high-finesse optical cavity (14) and is shared by both Yb systems. Light is frequency-shifted into resonance with the clock transition of each atomic system by independent acousto-optic modulators (AOMs). Resonance is detected by monitoring the 1S_0 ground state population (N_g) and 3P_0 excited state population (N_e). A laser cycles ground state atoms on the 1S_0 - 1P_1 transition while a photomultiplier tube (PMT) collects the fluorescence, giving a measure of N_g . After 5-10 ms of cycling, these atoms are laser-heated out of the lattice. At this point, N_e is optically pumped to the lowest-lying 3D_1 state which decays back to the ground state. The 1S_0 - 1P_1 transition is cycled again, now measuring N_e . Combining these measurements yields a normalized mean excitation $N_e/(N_e + N_g)$. During spectroscopy, special attention was paid to eliminating residual Stark shifts stemming from amplified spontaneous emission of the lattice lasers, to eliminating residual Doppler effects from mechanical vibrations of the apparatus correlated with the experimental cycle, and to controlling the cold collision shift due to atomic interactions within the lattice (19).

By measuring the normalized excitation while modulating the clock laser frequency by ± 3 Hz, an error signal is computed for each Yb system. Subsequently, independent microprocessors provide a digital frequency correction $f_{1,2}(t)$ to their respective AOMs, thereby maintaining resonance on the line center. In this way, though derived from the same LO, the individual laser frequencies for Yb-1 and Yb-2 are decoupled, and are instead determined by their respective atomic samples (for all but the shortest time scales). The frequency correction signals $f_{1,2}(t)$ are shown in Fig. 2A for a 5000 s interval. Because the experimental cycles for each clock system are unsynchronized and have different durations, $f_{1,2}(t)$ are interpolated to a common time base and subtracted to compute the frequency difference between Yb-1 and Yb-2, as shown in Fig. 2, B, C, and D. Measurements such as these were repeated several times for intervals of $\sim 15,000$ s, demonstrating a clock instability reaching 4×10^{-18} at 7500 s. While collecting data over a 90,000 s interval, we observed the instability curve in Fig. 3, shown as the total Allan deviation for a single Yb clock. Prior to data analysis, approximately 25% of the attempted measurement time was excluded due to laser unlocks and auxiliary servo failures (15). Each clock servo had an attack time of a

few seconds, evidenced by the instability bump near 3 s. At $\tau = 1\text{--}5$ s, the instability is comparable to previous measurements (14) of the free-running laser system, and at long times the instability averages down like white frequency noise as $\propto 3.2 \times 10^{-16} / \sqrt{\tau}$ (for averaging times τ in seconds), reaching 1.6×10^{-18} at 25,000 s.

Also shown in Fig. 3 is an estimate of the combined instability contribution (blue dashed) from the Dick effect and QPN (shaded region denotes the uncertainty of estimate). These contributions must be reduced if 10^{-18} instability is desired at timescales under 100 s. Significant reductions of QPN are possible by using higher atom numbers and longer interrogation times. Further stabilization of the optical LO will continue to reduce the Dick effect, by both lowering the laser frequency noise down-converted in the Dick process, and allowing increased spectroscopy times for higher duty cycles. Improved LOs will use optical cavities exhibiting reduced Brownian thermal-mechanical noise by exploiting cryogenic operation (20), crystalline optical coatings (21), longer cavities, or other techniques (14). Figure 4 demonstrates the advantage of improving the present LO, with four times less laser frequency noise and four times longer interrogation time (corresponding to a short-term laser instability $\sim 5 \times 10^{-17}$). The red dotted line gives the Dick instability, while the black dashed line indicates the QPN limit, assuming a moderate 50,000 atom number.

Noting that the calculated Dick effect remains several times higher than the QPN limit, we consider an alternative idea first proposed for microwave ion clocks: interleaved interrogation of two atomic systems (13). By monitoring the LO laser frequency at all times with interleaved atomic systems, the aliasing problem at the heart of the Dick effect can be highly suppressed. The solid blue line in Fig. 4 illustrates the potential of a simple interleaved-clock interrogation using Ramsey spectroscopy. Even using the present LO, the Dick effect is decreased well below the QPN limit afforded by a much improved LO (black dashed line). In this case, spin squeezing of the atomic sample could reduce the final instability beyond the standard quantum limit set by QPN [e.g., (22)]. The two-system, interleaved technique requires spectroscopy times that last one half or more of the total experimental cycle. By extending the Yb clock Ramsey spectroscopy time to >250 ms, we achieved a 50% duty cycle for each system, demonstrating the feasibility of this technique. Further suppression of the Dick effect can be achieved using a more selective interleaving scheme. Duty cycles $\geq 50\%$ can also be realized with the aid of nondestructive state detection (23).

Another important property of a clock is its accuracy, which results from uncertainty in systematic effects that alter a standard's periodicity from its natural, unperturbed state. In 2009, we completed a systematic analysis of Yb-1 at the 3×10^{-16} uncertainty level (16). Since then, we reduced the dominant uncertainty due to the blackbody Stark effect by an order of magnitude (24). With its recent construction, Yb-2 has not yet been systematically evaluated. The fact that the instability reaches the 10^{-18} level indicates that key systematic effects (e.g., blackbody Stark effect, atomic collisions, lattice light shifts) on each system are well-controlled over the relevant timescales. The mean frequency difference in Fig. 2 was $\langle f_2(t) - f_1(t) \rangle = -30$ mHz, which is within the Yb-1 uncertainty at 10^{-16} . Systematic effects on each system can now be efficiently characterized beyond the 10^{-17} -level. With continued progress, we envision 10^{-18} instability in only 100 s and long-term instability well below 10^{-18} .

Clock measurement at the 10^{-18} -level can be used to resolve spatial and temporal fluctuations equivalent to 1 cm of elevation in Earth's gravitational field (25–28), potentially impacting geodesy, hydrology, geology, and climate change studies. Space-based implementations can probe alternative gravitational theories, including red-shift deviations from general relativity with three orders of magnitude higher precision than at present (28). Though present-day temporal and spatial variation of fundamental constants is known to be small (6, 29, 30), 10^{-18} -level

clock measurements can offer tighter constraints. Finally, timekeeping improvements can benefit navigation systems, telescope array synchronization (e.g., VLBI), secure communication, interferometry, and possible redefinition of the SI second (9).

References and Notes

1. A. Bauch, Caesium atomic clocks: Function, performance and applications. *Meas. Sci. Technol.* **14**, 1159–1173 (2003). doi:10.1088/0957-0233/14/8/301
2. J. Levine, Introduction to time and frequency metrology. *Rev. Sci. Instrum.* **70**, 2567 (1999). doi:10.1063/1.1149844
3. S. A. Diddams, J. C. Bergquist, S. R. Jefferts, C. W. Oates, Standards of time and frequency at the outset of the 21st century. *Science* **306**, 1318–1324 (2004). doi:10.1126/science.1102330
4. J. Guena, M. Abgrall, D. Rovera, P. Laurent, B. Chupin, M. Lours, G. Santarelli, P. Rosenbusch, M. E. Tobar, Ruoxin Li, K. Gibble, A. Clairon, S. Bize, Progress in atomic fountains at LNE-SYRTE. *IEEE Trans. Ultra. Ferro. Freq. Cont.* **59**, 391–409 (2012). doi:10.1109/TUFFC.2012.2208
5. T. E. Parker, Long-term comparison of caesium fountain primary frequency standards. *Metrologia* **47**, 1–10 (2010). doi:10.1088/0026-1394/47/1/001
6. T. Rosenband, D. B. Hume, P. O. Schmidt, C. W. Chou, A. Brusch, L. Lorini, W. H. Oskay, R. E. Drullinger, T. M. Fortier, J. E. Stalnaker, S. A. Diddams, W. C. Swann, N. R. Newbury, W. M. Itano, D. J. Wineland, J. C. Bergquist, Frequency ratio of Al^+ and Hg^+ single-ion optical clocks; metrology at the 17th decimal place. *Science* **319**, 1808–1812 (2008). doi:10.1126/science.1154622
7. C. W. Chou, D. B. Hume, J. C. J. Koelemeij, D. J. Wineland, T. Rosenband, Frequency comparison of two high-accuracy Al^+ optical clocks. *Phys. Rev. Lett.* **104**, 070802 (2010). doi:10.1103/PhysRevLett.104.070802 Medline
8. T. L. Nicholson, M. J. Martin, J. R. Williams, B. J. Bloom, M. Bishof, M. D. Swallows, S. L. Campbell, J. Ye, Comparison of two independent Sr optical clocks with 1×10^{-17} stability at 10^3 s. *Phys. Rev. Lett.* **109**, 230801 (2012). doi:10.1103/PhysRevLett.109.230801 Medline
9. R. Le Targat, L. Lorini, Y. Le Coq, M. Zawada, J. Guéna, M. Abgrall, M. Gurov, P. Rosenbusch, D. G. Rovera, B. Nagórny, R. Gartman, P. G. Westergaard, M. E. Tobar, M. Lours, G. Santarelli, A. Clairon, S. Bize, P. Laurent, P. Lemonde, J. Lodewyck, Experimental realization of an optical second with strontium lattice clocks. *Nat. Commun.* **4**, 2109 (2013). doi:10.1038/ncomms3109
10. C. A. Greenhall, D. A. Howe, D. B. Percival, Total variance, an estimator of long-term frequency stability [standards]. *IEEE Trans. Ultra. Ferro. Freq. Cont.* **46**, 1183–1191 (1999). doi:10.1109/58.796124
11. W. M. Itano, J. C. Bergquist, J. J. Bollinger, J. M. Gilligan, D. J. Heinzen, F. L. Moore, M. G. Raizen, D. J. Wineland, Quantum projection noise: Population fluctuations in two-level systems. *Phys. Rev. A* **47**, 3554–3570 (1993). doi:10.1103/PhysRevA.47.3554 Medline
12. G. Santarelli, C. Audoin, A. Makdissi, P. Laurent, G. J. Dick, A. Clairon, Frequency stability degradation of an oscillator slaved to a periodically interrogated atomic resonator. *IEEE Trans. Ultra. Ferro. Freq. Cont.* **45**, 887–894 (1998). doi:10.1109/58.710548
13. G. J. Dick, J. D. Prestage, C. A. Greenhall, L. Maleki, *Proceedings of the 22nd Precise Time and Time Interval Meeting* (1990), pp. 487–508.
14. Y. Y. Jiang, A. D. Ludlow, N. D. Lemke, R. W. Fox, J. A. Sherman, L.-S. Ma, C. W. Oates, Making optical atomic clocks more stable with 10^{-16} -level laser stabilization. *Nat. Photonics* **5**, 158–161 (2011). doi:10.1038/nphoton.2010.313
15. See supplementary materials online.
16. N. D. Lemke, A. D. Ludlow, Z. W. Barber, T. M. Fortier, S. A. Diddams, Y. Jiang, S. R. Jefferts, T. P. Heavner, T. E. Parker, C. W. Oates, Spin-1/2 optical lattice clock. *Phys. Rev. Lett.* **103**, 063001 (2009). doi:10.1103/PhysRevLett.103.063001 Medline
17. J. Ye, H. J. Kimble, H. Katori, Quantum state engineering and precision metrology using state-insensitive light traps. *Science* **320**, 1734–1738 (2008). doi:10.1126/science.1148259
18. H. Katori, M. Takamoto, V. G. Pal'chikov, V. D. Ovsiannikov, Ultrastable optical clock with neutral atoms in an engineered light shift trap. *Phys. Rev. Lett.* **91**, 173005 (2003). doi:10.1103/PhysRevLett.91.173005 Medline
19. N. D. Lemke, J. von Stecher, J. A. Sherman, A. M. Rey, C. W. Oates, A. D. Ludlow, p-wave cold collisions in an optical lattice clock. *Phys. Rev. Lett.* **107**, 103902 (2011). doi:10.1103/PhysRevLett.107.103902 Medline

20. T. Kessler, C. Hagemann, C. Grebing, T. Legero, U. Sterr, F. Riehle, M. J. Martin, L. Chen, J. Ye, A sub-40-mHz-linewidth laser based on a silicon single-crystal optical cavity. *Nat. Photonics* **6**, 687–692 (2012). [doi:10.1038/nphoton.2012.217](https://doi.org/10.1038/nphoton.2012.217)
21. G. D. Cole, W. Zhang, M. J. Martin, J. Ye, M. Aspelmeyer, available at <http://arxiv.org/abs/1302.6489> (2013).
22. I. D. Leroux, M. H. Schleier-Smith, V. Vuletić, Implementation of cavity squeezing of a collective atomic spin. *Phys. Rev. Lett.* **104**, 073602 (2010). [doi:10.1103/PhysRevLett.104.073602](https://doi.org/10.1103/PhysRevLett.104.073602)
23. P. G. Westergaard, J. Lodewyck, P. Lemonde, Minimizing the dick effect in an optical lattice clock. *IEEE Trans. Ultra. Ferro. Freq. Cont.* **57**, 623–628 (2010). [doi:10.1109/TUFFC.2010.1457](https://doi.org/10.1109/TUFFC.2010.1457)
24. J. A. Sherman, N. D. Lemke, N. Hinkley, M. Pizzocaro, R. W. Fox, A. D. Ludlow, C. W. Oates, High-accuracy measurement of atomic polarizability in an optical lattice clock. *Phys. Rev. Lett.* **108**, 153002 (2012). [doi:10.1103/PhysRevLett.108.153002](https://doi.org/10.1103/PhysRevLett.108.153002) [Medline](#)
25. S. Schiller, A. Görlitz, A. Nevsky, J. C. J. Koelemeij, A. Wicht, P. Gill, H. A. Klein, H. S. Margolis, G. Miletì, U. Sterr, F. Riehle, E. Peik, C. Tamm, W. Ertmer, E. Rasel, V. Klein, C. Salomon, G. M. Tino, P. Lemonde, R. Holzwarth, T. W. Hänsch, Optical clocks in space. *Nucl. Phys. B Proc. Suppl.* **166**, 300–302 (2007). [doi:10.1016/j.nuclphysbps.2006.12.032](https://doi.org/10.1016/j.nuclphysbps.2006.12.032)
26. C. W. Chou, D. B. Hume, T. Rosenband, D. J. Wineland, Optical clocks and relativity. *Science* **329**, 1630–1633 (2010). [doi:10.1126/science.1192720](https://doi.org/10.1126/science.1192720)
27. D. Kleppner, Time too good to be true. *Phys. Today* **59**, 10 (2006). [doi:10.1063/1.2195297](https://doi.org/10.1063/1.2195297)
28. S. Schiller, G. M. Tino, P. Gill, C. Salomon, U. Sterr, E. Peik, A. Nevsky, A. Görlitz, D. Svehla, G. Ferrari, N. Poli, L. Lusanna, H. Klein, H. Margolis, P. Lemonde, P. Laurent, G. Santarelli, A. Clairon, W. Ertmer, E. Rasel, J. Müller, L. Iorio, C. Lämmerzahl, H. Dittus, E. Gill, M. Rothacher, F. Flechner, U. Schreiber, V. Flambaum, W.-T. Ni, L. Liu, X. Chen, J. Chen, K. Gao, L. Cacciapuoti, R. Holzwarth, M. P. Heß, W. Schäfer, Einstein Gravity Explorer—A medium-class fundamental physics mission. *Exp. Astron.* **23**, 573–610 (2009). [doi:10.1007/s10686-008-9126-5](https://doi.org/10.1007/s10686-008-9126-5)
29. T. Chiba, The constancy of the constants of nature: Updates. *Prog. Theor. Phys.* **126**, 993–1019 (2011). [doi:10.1143/PTP.126.993](https://doi.org/10.1143/PTP.126.993)
30. S. Blatt, A. D. Ludlow, G. K. Campbell, J. W. Thomsen, T. Zelevinsky, M. M. Boyd, J. Ye, X. Baillard, M. Fouché, R. Le Targat, A. Brusch, P. Lemonde, M. Takamoto, F. L. Hong, H. Katori, V. V. Flambaum, New limits on coupling of fundamental constants to gravity using ⁸⁷Sr optical lattice clocks. *Phys. Rev. Lett.* **100**, 140801 (2008). [doi:10.1103/PhysRevLett.100.140801](https://doi.org/10.1103/PhysRevLett.100.140801) [Medline](#)

Acknowledgments: The authors acknowledge DARPA QuASAR, NASA Fundamental Physics, and NIST for financial support, D. Hume for experimental assistance, and T. Fortier and S. Diddams for femtosecond optical frequency comb measurements.

Supplementary Materials

www.sciencemag.org/cgi/content/full/science.1240420/DC1

Supplementary Text

Table S1

13 May 2013; accepted 12 August 2013

Published online 22 August 2013

10.1126/science.1240420

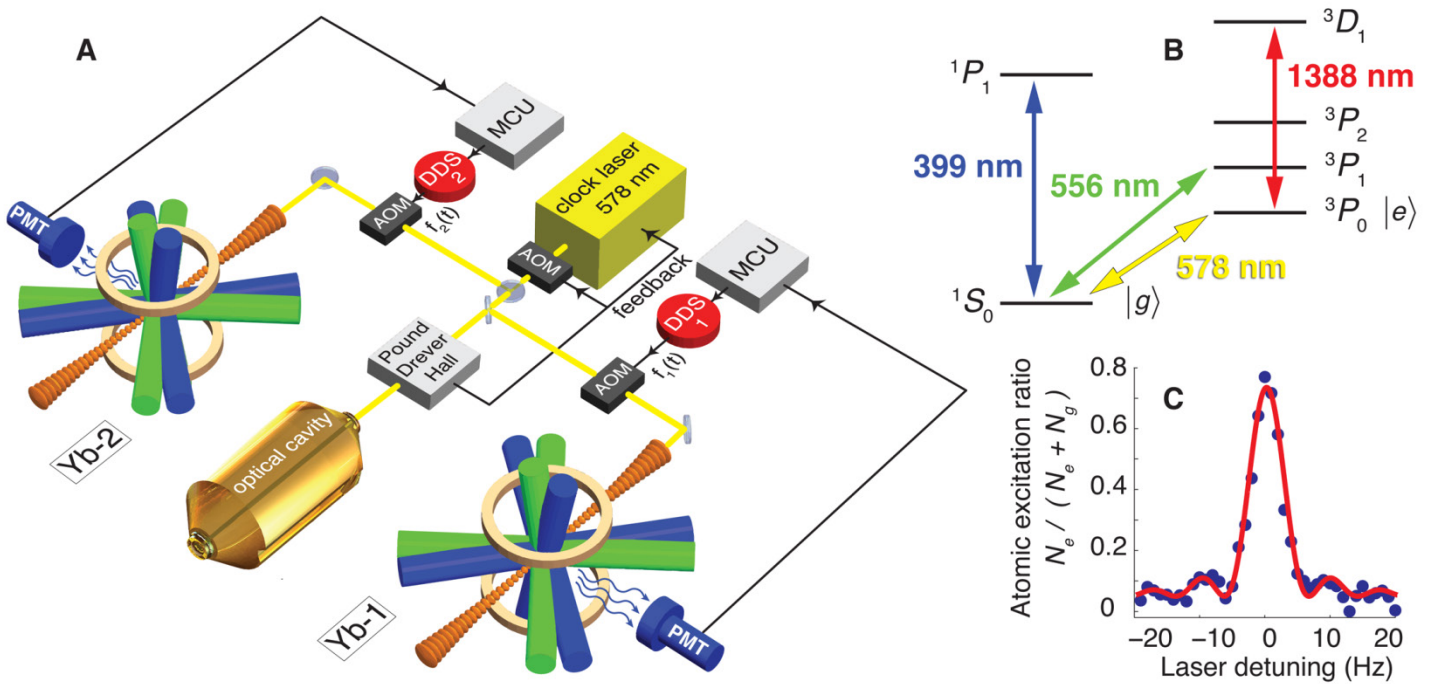


Fig. 1. (A) Laser light at 578 nm is pre-stabilized to an isolated, high-finesse optical cavity using Pound-Drever-Hall detection and electronic feedback to an acousto-optic modulator (AOM) and laser piezoelectric-transducer. Fibers deliver stabilized laser light to the Yb-1 and Yb-2 systems. Resonance with the atomic transition is detected by observing atomic fluorescence collected onto a photomultiplier tube (PMT). The fluorescence signal is digitized and processed by a microcontroller unit (MCU), which computes a correction frequency, $f_{1,2}(t)$. This correction frequency is applied to the relevant AOM by way of a direct digital synthesizer (DDS), and locks the laser frequency onto resonance with the clock transition. (B) Relevant Yb atomic energy levels and transitions, including laser cooling transitions (399 and 556 nm), the clock transition (578 nm), and the optical pumping transition used for excited state detection (1388 nm). (C) A single-scan, normalized excitation spectrum of the 1S_0 - 3P_0 clock transition in ^{171}Yb with 140 ms Rabi spectroscopy time; the red line is a free-parameter sinc^2 function fit.

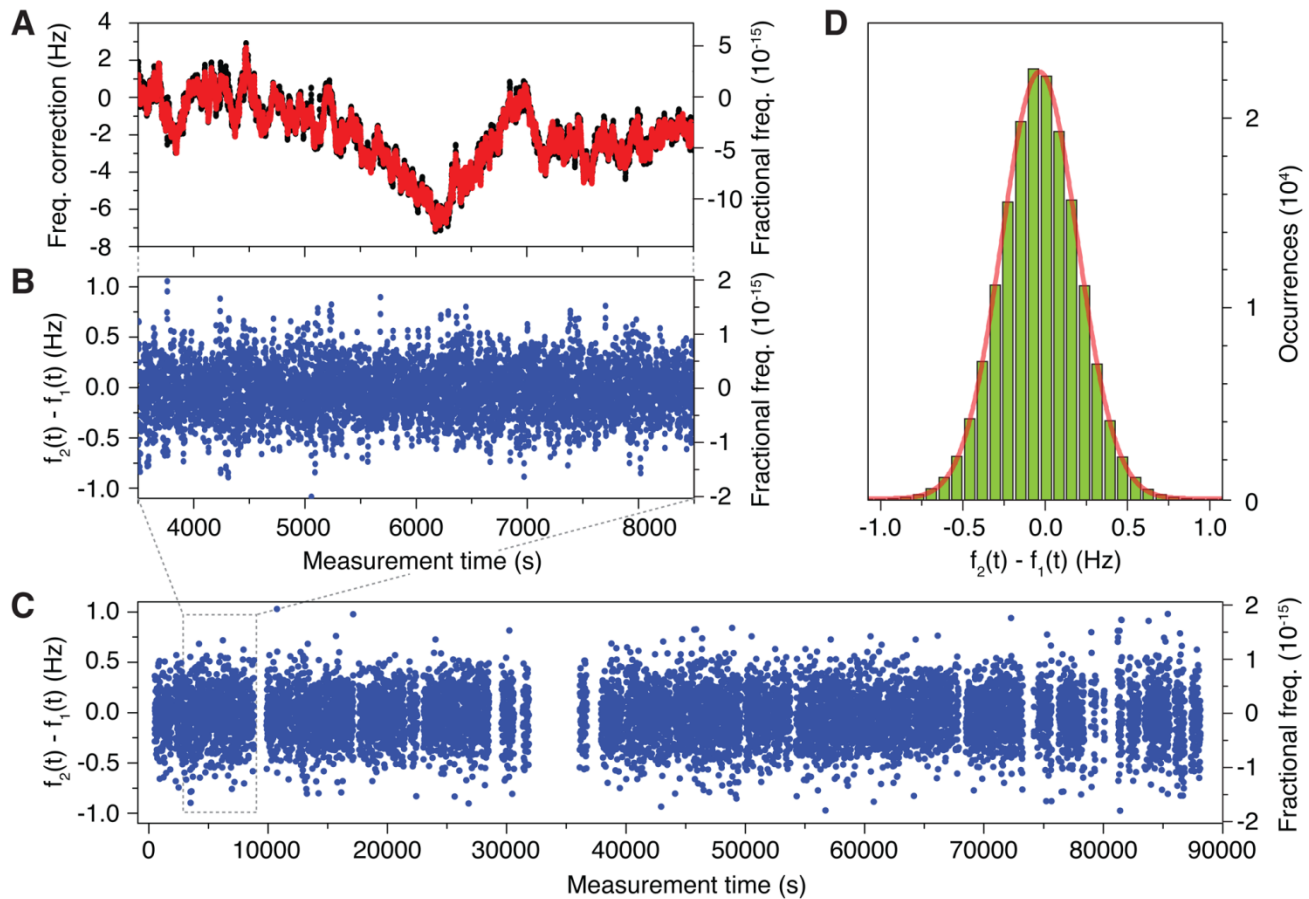


Fig. 2. (A) Correction frequencies, $f_{1,2}(t)$, are shown in red and black. Dominant LO fluctuations are due to the cavity and are thus common to the atomic systems. (B) Frequency difference between the two Yb clock systems, $f_2(t) - f_1(t)$, for a 5000 s interval. (C) Data set $f_2(t) - f_1(t)$ over a 90,000 s interval. Gaps represent data rejected before data analysis due to servo unlocks. (D) A histogram of all data and a Gaussian fit ($\chi_r^2 = 0.9996$).

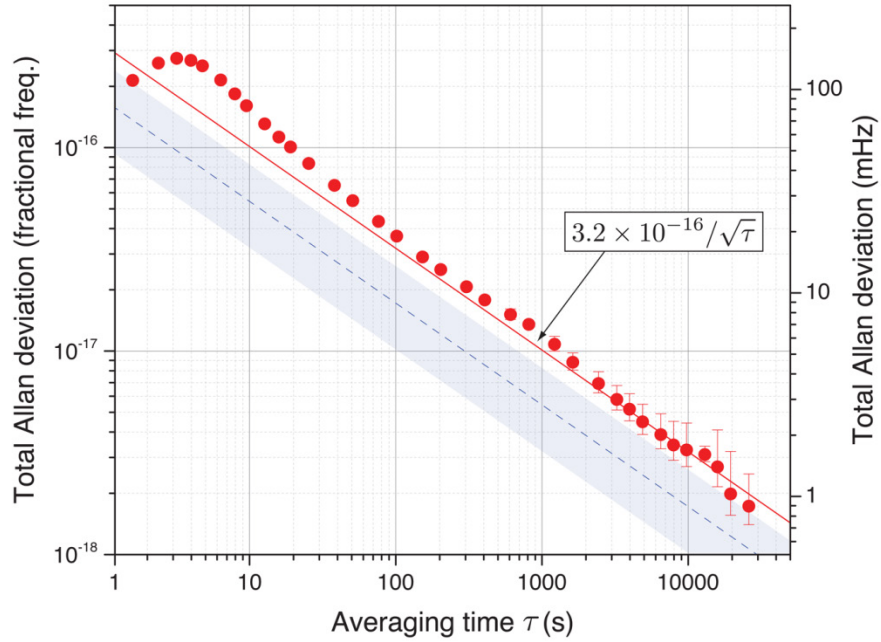


Fig. 3. Total Allan deviation of a single Yb clock, $(f_2(t) - f_1(t))/\sqrt{2}$ (red circles), and its white-frequency-noise asymptote of $3.2 \times 10^{-16}/\sqrt{\tau}$ (red solid line). The blue dashed line represents the estimated combined instability contributions from the Dick effect ($1.4 \times 10^{-16}/\sqrt{\tau}$) and QPN ($1 \times 10^{-16}/\sqrt{\tau}$); the shaded region denotes uncertainty in these estimates.

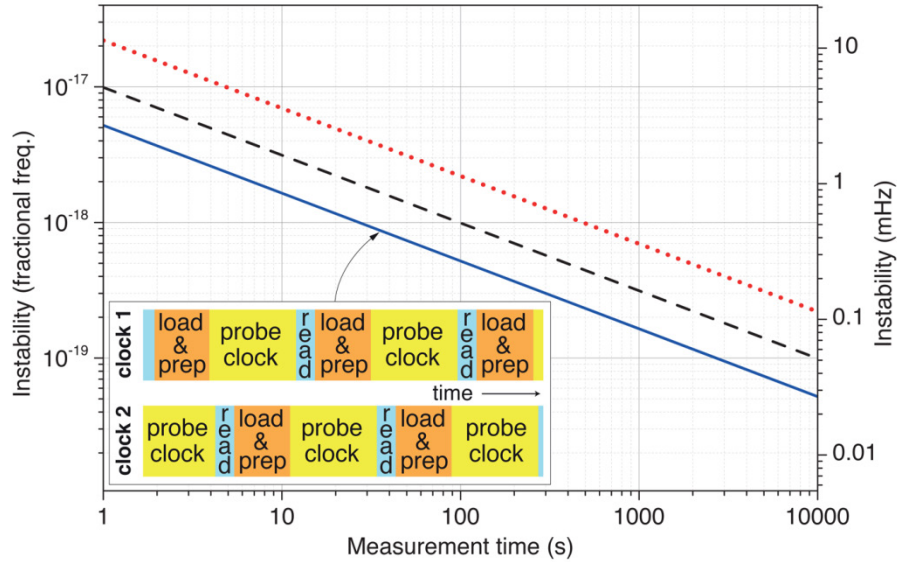


Fig. 4. Calculated instability limits toward the goal of 1×10^{-18} in 100 s. The Dick limit (red dotted) is reduced by using a LO which is four times as stable than used here. The QPN limit is shown under the same conditions (black dashed) assuming 50,000 atoms. The inset illustrates an interleaved interrogation of two atomic systems, allowing continuous monitoring of the LO for suppression of the Dick effect. Dead times from atomic preparation or readout in one system are synchronized with clock interrogation in the second system. The solid blue line indicates the suppressed Dick instability in the interleaved-interrogation scheme using Ramsey spectroscopy with an unimproved LO.